Biochemical and Biophysical Research Communications 470 (2016) 15–21

Contents lists available at ScienceDirect

Biochemical and Biophysical Research Communications

journal homepage: www.elsevier.com/locate/ybbrc

DSS colitis promotes tumorigenesis and fibrogenesis in a choline-deficient high-fat diet-induced NASH mouse model

Koichi Achiwa [a], Masatoshi Ishigami [a, *], Yoji Ishizu [a], Teiji Kuzuya [a], Takashi Honda [a], Kazuhiko Hayashi [a], Yoshiki Hirooka [a], Yoshiaki Katano [b], Hidemi Goto [a]

[a] Department of Gastroenterology and Hepatology, Nagoya University Graduate, School of Medicine, Nagoya, Japan
[b] Department of Internal Medicine, Banbuntane Hotokukai Hospital, Fujita Health University, School of Medicine, Nagoya, Japan

ARTICLE INFO

Article history:
Received 24 November 2015
Accepted 2 December 2015
Available online 10 December 2015

Keywords:
Tumorigenesis
Fibrosis
Choline-deficient high-fat
Nonalcoholic steatohepatitis
Colitis

ABSTRACT

Nonalcoholic steatohepatitis (NASH) patients progress to liver cirrhosis and even hepatocellular carcinoma (HCC). Several lines of evidence indicate that accumulation of lipopolysaccharide (LPS) and disruption of gut microbiota play contributory roles in HCC. Moreover, in a dextran sodium sulfate (DSS)-induced colitis model in mice, a high-fat diet increases portal LPS level and promotes hepatic inflammation and fibrosis. However, this diet-induced NASH model requires at least 50 weeks for carcinogenesis. In this study, we sought to determine whether increased intestinal permeability would aggravate liver inflammation and fibrosis and accelerate tumorigenesis in a diet-induced NASH model. Mice were fed a choline-deficient high-fat (CDHF) diet for 4 or 12 weeks. The DSS group was fed CDHF and intermittently received 1% DSS in the drinking water. Exposure to DSS promoted mucosal changes such as crypt loss and increased the number of inflammatory cells in the colon. In the DSS group, portal LPS levels were elevated at 4 weeks, and the proportions of *Clostridium cluster* XI in the fecal microbiota were elevated. In addition, levels of serum transaminase, number of lobular inflammatory cells, F4/80 staining–positive area, and levels of inflammatory cytokines were all elevated in the DSS group. Liver histology in the DSS group revealed severe fibrosis at 12 weeks. Liver tumors were detected in the DSS group at 12 weeks, but not in the other groups. Thus, DSS administration promoted liver tumors in a CDHF diet-induced NASH mouse over the short term, suggesting that the induction of intestinal inflammation and gut disruption of microbiota in NASH promote hepatic tumorigenesis.

1. Introduction

Nonalcoholic fatty liver disease (NAFLD) covers a spectrum of conditions ranging from simple hepatic steatosis to nonalcoholic steatohepatitis (NASH), ultimately leading to cirrhosis and hepatocellular carcinoma (HCC) [1,2]. The prevalence of NAFLD has increased in recent years [3].

The pathogenesis of NASH is not well understood, although the 'two-hit' hypothesis is widely accepted [4]. Obesity, hypertension, hyperglycemia, and diabetes mellitus are key factors in development of the first hit. Once hepatic steatosis is established, the liver becomes susceptible to a second hit, such as oxidative stress, iron deposition, endotoxin, mitochondrial dysfunction, lipid peroxidation, or pro-inflammatory cytokines [5–7].

A number of animal models have been developed for the study of NAFLD or NASH. Three representative feeding regimens induce NAFLD/NASH in mice: methionine/choline-deficient (MCD), choline-deficient (CD), and high-fat (HF) diets. However, none of them are complete models of human NASH. The MCD diet model does not have long-term survival and causes weight loss; the CD diet model causes only slight hepatic inflammation and fibrosis;

Abbreviation: NASH, nonalcoholic steatohepatitis; HCC, hepatocellular carcinoma; LPS, lipopolysaccharide; DSS, dextran sodium sulfate; CDHF, choline-deficient high-fat; NAFLD, nonalcoholic fatty liver disease; AST, aspartate transaminase; ALT, alanine aminotransferase; MCD, methionine/choline-deficient; CD, choline-deficient; SMA, smooth muscle actin; HSC, hepatic stellate cell; TGF, transforming growth factor.

* Corresponding author. Department of Gastroenterology and Hepatology, Nagoya University Graduate School of Medicine, 65 Tsuruma-cho, Showa-ku, Nagoya 466-8550, Japan.
E-mail address: masaishi@med.nagoya-u.ac.jp (M. Ishigami).

http://dx.doi.org/10.1016/j.bbrc.2015.12.012
0006-291X/

and the HF diet model does not cause inflammation or fibrosis [8]. Therefore, we combined the CD and HF diets and used the resultant choline-deficient high-fat (CDHF) diet to induce NASH. Previous work showed that long-term exposure to a CDHF diet leads to cancer in mice [9].

Multiple studies have confirmed that bacterial flora are altered and intestinal permeability is elevated in NAFLD/NASH and liver cirrhosis [10–12]. Furthermore, in these conditions, endotoxin enters the liver through the portal vein and enhances liver damage, thereby stimulating Kupffer cells (liver-resident macrophages) [13]. A recent report demonstrated that disruption of intestinal microbiota and accumulation of endotoxin leads to mediating accelerated proliferation, expression of the hepatomitogen epiregulin, and prevention of apoptosis, all of which promote HCC development [14,15]. Exposure to DSS (dextran sulfate sodium) leads to intestinal permeability and mucosal changes in the ileum and colon [16,17]. Intestinal inflammation causes release of pro-inflammatory cytokines from intestinal cells, which may also contribute to the development of HCC in patients with chronic inflammatory liver disease. However, the involvement of gut homeostasis in inflammation-associated HCC has not been explored. Therefore, we investigated whether increased intestinal permeability would aggravate liver inflammation and fibrosis and lead to tumorigenesis in a diet-induced NASH model.

2. Materials and methods

2.1. Animals and treatment

Male 20-week-old C57/BL6 mice were purchased from SLC Japan (Shizuoka, Japan). Mice were fed a choline-deficient high-fat (CDHF) diet; chow was purchased from Oriental Yeast (Tokyo, Japan). In parallel experiments, mice were exposed to 1% DSS (M.W. = 36,000–50,000; MP Biomedicals, Solon, OH, USA) in the drinking water, leading to increased intestinal permeability and mucosal changes in the colon. DSS was applied in cycles; each cycle consisted of 7 days of DSS administration followed by a 10-day interval with normal drinking water. Mice (N = 8 or 12 per subgroup) were sacrificed after 4 or 12 weeks of treatment, and samples were processed for histopathology. During the experiment, body weight was measured weekly. Mice were maintained at 23 ± 1°C with a 12:12 h light/dark cycle, humidity 50 ± 10%. The procedures employed for the handling and care of animals were approved by the Animal Experiment Committee, Nagoya University, and conformed to the national guidelines for animal usage in research.

2.2. General tissue preparation

Blood was taken from the portal vein at the time of sacrifice after a 12-h fast. Serum was obtained by centrifugation at 3000 × *g* for 15min. Mice were anesthetized by intraperitoneal injection of pentobarbital. Liver and colon were resected for histological analysis.

2.3. Biochemical analysis

Total protein, albumin, total bilirubin, triglycerides total cholesterol, aspartate transaminase (AST), alanine aminotransferase (ALT), and glucose were measured by SRL (Tokyo, Japan).

2.4. Endotoxin assay

LPS was measured in serum using the limulus amebocyte lysate (LAL) assay (QCL-1000 Test Kit, LONZA). Blood samples were collected from the portal vein; after centrifugation (4000 × *g*, 5 min), plasma was transferred into LPS-free cups and stored at −20 °C until analysis. Following testing, samples were mixed with LAL and the chromogenic substrate reagent, incubated for 16 min, and measured on a plate reader capable of measuring absorbance at 405–410 nm.

2.5. Bacterial load assay

Fecal samples were obtained from colons on the day of sacrifice, frozen, and stored at −70 °C. DNA was extracted, and bacterial 16S ribosomal RNA genes were amplified using specific primers and measured by T-RFLP (Terminal Restriction Fragment Length Polymorphism) analysis as described by Nagashima et al. [18–20].

2.6. Histology and immunohistochemistry

Hepatic tissue and colons from mice of each group were removed and fixed in 4% paraformaldehyde in phosphate-buffered saline, and then embedded in paraffin. Hepatic sections (3 μm thick) and colon sections (7 μm thick) were cut from paraffin blocks for staining with hematoxylin & eosin and Sirius red (Sigma–Aldrich, St. Louis, MO, USA) for histological examination. For immunohistochemistry, samples were incubated overnight at 22°C with anti-F4/80 antibody (ab111101, 1:100, Abcam, Tokyo, Japan). After incubation with appropriate the DAKO Envision Labeled Polymer Anti-Rabbit system (Dako Cytomation, Tokyo, Japan). Antigen retrieval was performed by heating for 15 min in a microwave. For quantitative analysis of hepatic steatosis, Sirius red– and F4/80-positive areas were captured and measured in 10 microscopic fields for each tissue section at 200-fold magnification, using the BZ-II Image Analysis Application (KEYENCE, Osaka, Japan). For the calculation, parts of the vessel area and vessel wall were excluded. Histological evaluation of colitis was performed using a previously described histological score, which was determined according to the following histological criteria [21].

2.7. Lipid isolation and measurement

Hepatic triglyceride, total cholesterol, and free cholesterol were measured using the Triglyceride E, Cholesterol E, and Free Cholesterol E kits (Wako, Osaka, Japan).

2.8. Quantitative real-time polymerase chain reaction analysis

Total RNA was extracted from liver tissues using Trizol (Life Technologies, Tokyo, Japan). Reverse transcription of total RNA for cDNA synthesis was synthesized using the Revertra-Ace qPCR-RT kit (TOYOBO, Osaka, Japan). Gene expression was analyzed by TaqMan real-time quantitative polymerase chain reaction (qPCR) on an MX3005P sequence detection system (Agilent Technologies, Tokyo, Japan). Samples were measured in duplicate. Amplification conditions were as follows: 1 cycle of 95 °C for 3 min, followed by 40 cycles of 95°C for 10 s and 60°C for 22 s. Primers were as follows: Interleukin 6, IL-6 (Mm00446190), Interleukin 1 beta, IL-1β (Mm00434228), EGF-like module containing, mucin-like hormone receptor-like1, EMR1 (Mm00802530), transforming growth factor beta 1, TGF-β1 (Mm03024053), smooth muscle α-actin, α-SMA (Mm01546133), inducible nitric oxide synthase, iNOS (Mm00440502), Mitogen-activated protein kinase 8, MAPK8 (Mm00489514), and hypoxanthine guanine phosphoribosyl transferase, HPRT (Mm00446968). Expression of each target sequence was normalized to the corresponding level of HPRT mRNA.

2.9. Statistical analysis

All statistical analyses were performed using the Statistical Package for Social Sciences (SPSS), version 22. Data were presented as bar graphs showing means ± SEM. Statistical analysis was performed using Student's t test. When the p value was less than 0.05, differences were considered to be statistically significant.

3. Results

3.1. Changes in body weight and liver-to-body weight ratio after DSS and CDHF diet administration

Body weight changes between the two groups are summarized in Table 1.CDHF diet–fed mice slightly increased their body weight throughout the experimental period. DSS treatment caused a decrease of body weight at 12 weeks, but weight at 4 weeks did not differ between the two groups. Liver and body weight ratio was higher in the CDHF + DSS group than in the CDHF group after 4 and 12 weeks.

3.2. Administration of DSS causes intestinal inflammation and increases the level of portal LPS

Histological changes in the colon were found in both groups. Exposure of DSS led to increase mucosal changes such as crypt loss and an increase in the number of inflammatory cells in the colon (Fig. 1A). The CDHF + DSS group had shorter colons than the CDHF group (Fig. 1B).

Accordingly, the histological scores were significantly higher in the CDHF + DSS group than in the CDHF group (Fig. 1C). However, a few colon tissues from the CDHF group exhibited increased numbers of inflammatory cells at 4 and 12 weeks. The CDHF diet led to a slight increase in intestinal inflammation.

Portal LPS concentrations were analyzed by limulus amebocyte lysate (LAL) assay. LPS levels were higher in the CDHF + DSS group than in the CDHF group at 4 weeks, but there was no significant difference between groups at 12 weeks (Fig. 1D).

3.3. Disruption of gut homeostasis after CDHF and CDHF + DSS administration

Examination of gut microbiota by T-RFLP after CDHF and CDHF + DSS administration revealed that the composition of gut microbiota differed significantly between 4 and 12 weeks (Fig. 1E). The proportion of others in the CDHF + DSS group at 12 weeks was lower than that in the other groups. The variation of gut microbiota was reduced in the CDHF + DSS group at 12 weeks.

3.4. Hepatic steatosis and lipid accumulation after DSS and CDHF diet administration

CDHF + DSS–treated mice exhibited increases in serum and hepatic triglyceride and cholesterol relative to CDHF-treated mice at 4 weeks (Table 1). However, there was no significant difference in hepatic triglyceride or total and free cholesterol between the two groups at 12 weeks. Both groups exhibited severe macrovesicular steatosis in liver histology. Image analysis revealed no significant difference in lipid droplets between the two groups (date not shown). DSS administration had no effect on hepatic lipids at 12 weeks.

3.5. Administration of DSS enhances CDHF diet-induced liver damage and inflammation

Serum total bilirubin levels were significantly higher in the CDHF + DSS group than in the CDHF group. Serum transaminase levels were markedly higher in the CDHF + DSS group at both 4 and 12 weeks (Table 1).

We evaluated the degree of hepatic inflammation of the parenchyma by HE staining (Fig. 2A). A large number of lobular necroinflammatory cells were seen in the DSS group. Next, we performed F4/80 immunohistochemical staining, which indicates activation of inflammatory macrophages. Image analysis revealed significant elevation of F4/80 staining–positive area in the CDHF + DSS group relative to the CDHF group at both 4 and 12 weeks (Fig. 2B)

In addition, CDHF + DSS–treated mice at 4 weeks expressed higher levels of genes related to liver injury and inflammation, such as IL-1β and EMR1 (Fig. 2E, F). By contrast, mRNA expression of

Table 1
CDHF diet + DSS induced liver injury and steatosis in mice.

	4W		12W	
	CDHF(n = 8)	CDHF + DSS(n = 8)	CDHF(n = 12)	CDHF + DSS(n = 11)
Body weight(g)	24.02 ± 0.31	23.04 ± 0.31	25.20 ± 0.49	22.28 ± 1.36
Liver/body weight(%)	5.34 ± 0.19	7.22 ± 0.38*	7.22 ± 0.21	8.91 ± 0.47**
Serum				
Total Protein(g/dl)	5.03 ± 0.16	4.73 ± 0.46	4.76 ± 0.17	4.48 ± 1.03
Albumin (g/dl)	2.96 ± 0.08	2.62 ± 0.12	2.90 ± 0.16	2.67 ± 0.345
Total Bilirubin(mg/dl)	0.05 ± 0.009	0.15 ± 0.02*	0.13 ± 0.035	0.29 ± 0.166**
AST (IU/L)	132.5 ± 37.44	33221.62 ± 35.23*	233.62 ± 13.09	547.00 ± 42.83**
ALT (IU/L)	181.75 ± 24.94	463.00 ± 54.45*	251.62 ± 23.29	545.42 ± 45.90**
Glucose (mg/dl)	67.87 ± 12.64	55.85 ± 29.92	67.87 ± 12.64	55.85 ± 29.92
Triglyceride(mg/dl)	23.50 ± 2.51	41.37 ± 3.06*	40.00 ± 6.00	36.40 ± 13.97
Total cholesterol (mg/dl)	54.28 ± 1.45	66.25 ± 4.33*	56.25 ± 8.24	51.60 ± 38.70
Hepatic tissue				
Triglyceride (mg/g tissue)	214.95 ± 10.54	319.38 ± 6.55*	187.91 ± 29.11	185.19 ± 44.16
Total cholesterol (mg/g tissue)	11.32 ± 1.94	19.8 ± 3.28*	16.63 ± 3.10	17.85 ± 5.37

Data are mean ± SEM.
*p < 0.05 compared with CDHF diet group at 4W.
**p < 0.05 compared with CDHF diet group at 12W.
ALT, alanine aminotransferase; AST, aspartate aminotransferase.

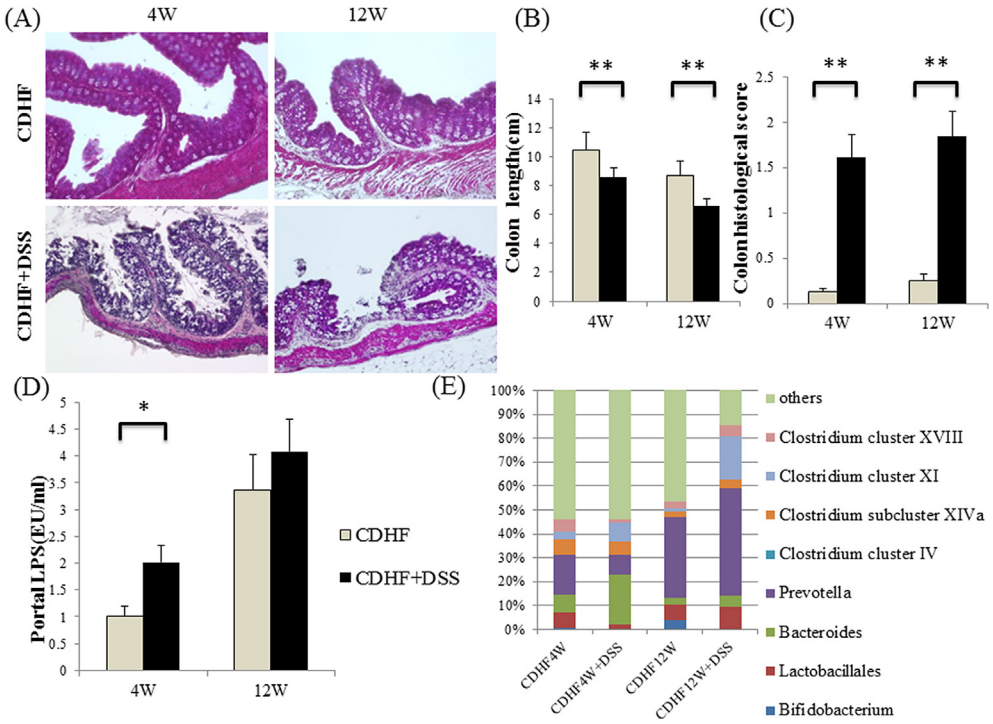

Fig. 1. Colon histology was evaluated by hematoxylin-eosin (HE) staining (× 200); representative histological observations are shown (A). Colon length (B) and colon histological score (C) were determined. Portal LPS levels (D) were determined.The proportions of fecal bacteria in the four groups were measured by T-RFLP (E). *P<0.05, **P<0.001.

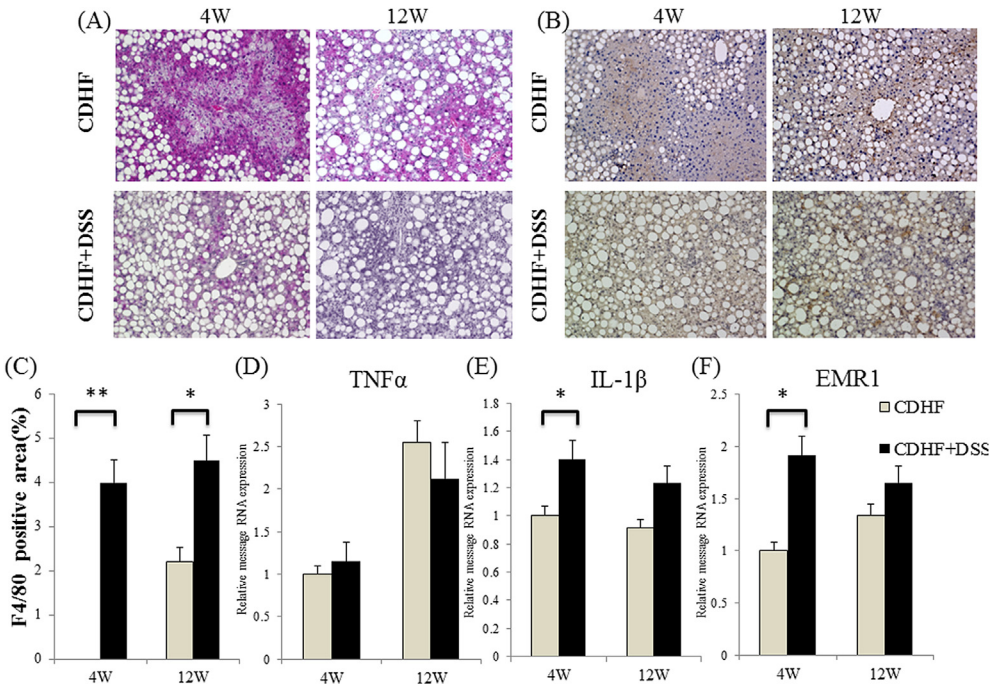

Fig. 2. Liver histology was evaluated by hematoxylin-eosin (HE) staining (× 200); representative histological observations are shown. Both CDHF and CDHF + DSS mice developed pathological NASH at 12 weeks, whereas CDHF mice did not develop NASH at 4 weeks (A). F4/80 immunohistochemical staining, which indicates activation of inflammatory macrophages, was analyzed (× 200) (B). Percentage of stained F4/80 positive area in each section was calculated as target area divided by whole area using the BZ-Analyzer-II imaging analysis software (C). Relative mRNA expression levels of TNFα, IL-1β, and EMR1 were determined (D, E, F). *P<0.05, **P < 0.001.

TNFα and iNOS did not differ significantly between groups at 4 weeks (Fig. 2D and 4)D.

3.6. Administration of DSS promoted CDHF diet-induced hepatic fibrosis

Fibrosis was detected by Sirius red staining. Both groups exhibited fibrosis in the perisinusoidal area and portal and

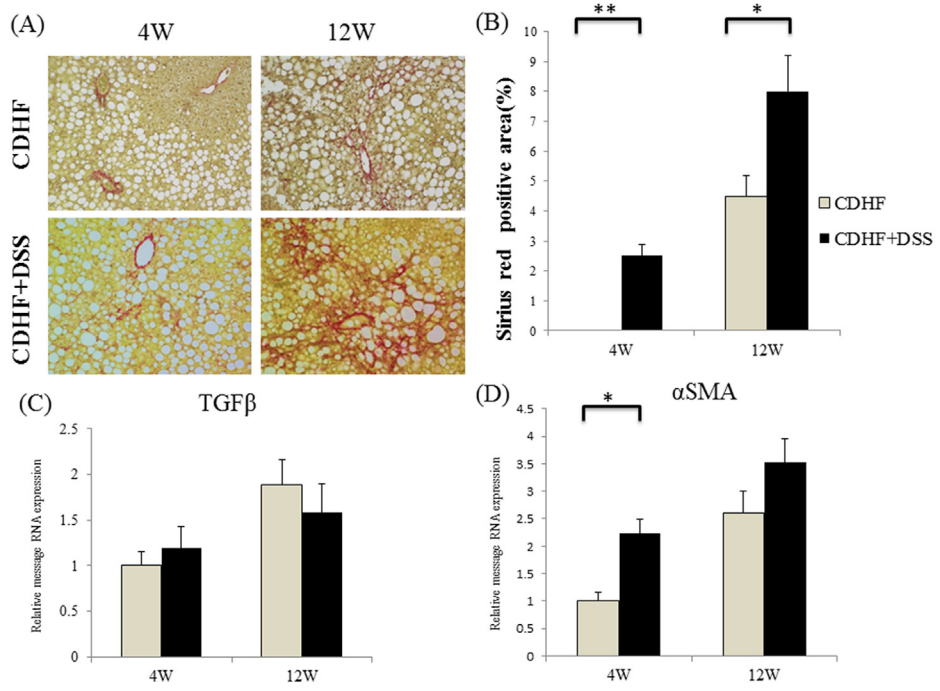

Fig. 3. Hepatic fibrosis was measured by Sirius red staining; representative histological observations are shown (A). Proportion of Sirius red−positive area in each section was calculated as target area divided by whole area using the BZ-Analyzer-II imaging analysis software (B). Relative mRNA expression of TGFβ (C) and α-SMA (D) were determined. *P<0.05 **P<0.001. (For interpretation of the references to colour in this figure legend, the reader is referred to the web version of this article.)

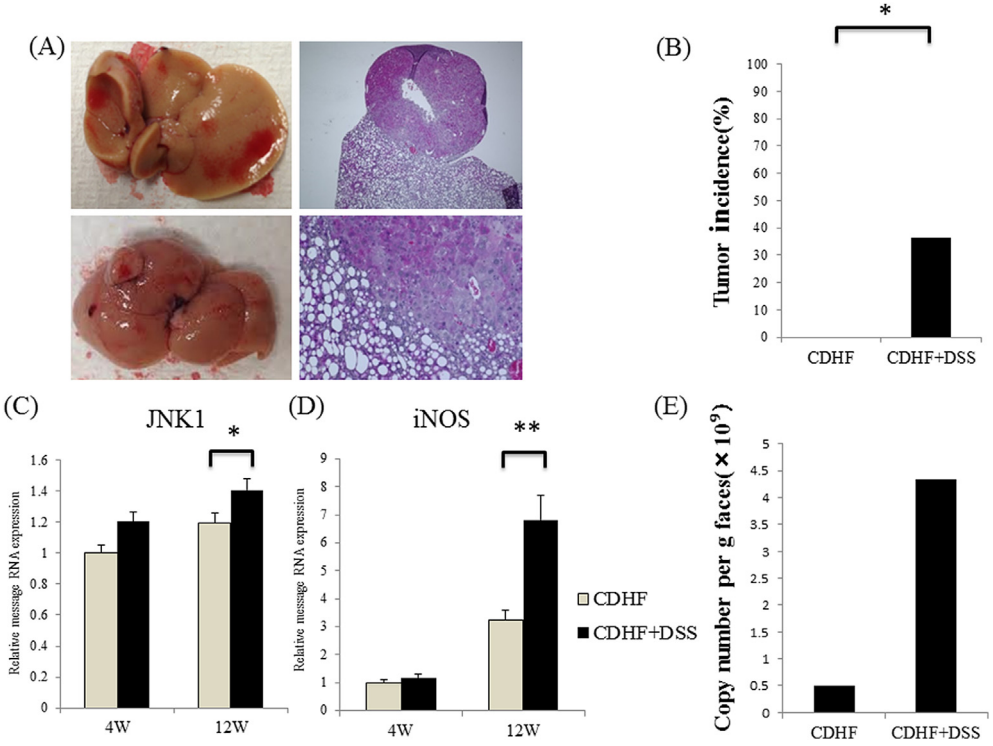

Fig. 4. Incidence of HCC in the CDHF + DSS group at 12 weeks. (A) Tumor incidence in surviving mice during the experimental period (B). Relative mRNA expression levels of JNK1 (C) and iNOS (D) were determined (P*<0.05). Quantitative real-time PCR of 16S rRNA genes demonstrated that the proportion of *Clostridium* cluster XI increased in the CDHF + DSS group at 12 weeks relative to the other groups (E).

periportal area at 12 weeks (Fig. 3A). However, the CDHF group did not exhibit fibrosis at 4 weeks. Image analysis revealed significant elevation of Sirius staining−positive area in the CDHF + DSS group at both time points. Next, we evaluated expression of genes related to fibrosis such as TGFβ and αSMA, a marker for activated hepatic stellate cells (HSCs). There was no significant difference in mRNA expression of TGFβ between groups at either time point (Fig. 3C). By contrast, mRNA expression of αSMA was significantly increased in the CDHF + DSS group relative to the CDHF group at 4 weeks (Fig. 3D).

3.7. Administration of DSS causes CDHF diet-induced early tumorigenesis

Five of sixteen mice in the DSS group died during the experimental period, and tumors were detected in 4 of the 11 surviving CDHF + DSS–treated mice at 12 weeks (Fig. 4B). One of the tumors was a highly differentiated HCC with clear boundaries and highly dysplastic cells with nuclear atypia (Fig. 4A). In the CDHF group, all mice survived, and no tumors were observed.

Expression of genes related to oxidative stress, such as iNOS, or hepatocyte proliferation, such as JNK1, was higher in the CDHF + DSS group at 12 weeks than in the other groups (Fig. 4C, D). T-RFLP analyses and quantitative real-time PCR of 16S rRNA genes demonstrated that the proportion of *Clostridium* cluster XI was higher in the CDHF + DSS group at 12 weeks than in the other groups (Fig. 4E).

4. Discussion

In this study, we observed tumors only in mice fed a CDHF diet with DSS for 12 weeks.

Very few studies have shown that HF diet alone promotes tumor development, and it takes 24–65 weeks to develop tumors in a CD diet model [22,23]. To address this issue, we established a diet-induced NASH model that induces tumorigenesis over a relatively short period. However, the mechanism of tumorigenesis in this NASH model remains to be elucidated. A CD diet induces peripheral hepatic insulin resistance [22] and ROS formation, lipid peroxidation, and mitochondrial dysfunction [24], all of which are associated with progression to NASH and HCC. In this study, iNOS mRNA expression was significantly higher in the CDHF + DSS group than in the CDHF group; this hepatic oxidative stress might be caused by DSS administration. Previous work showed that a CDHF diet alone requires a long period for tumor development [9].

A recent study showed that the gut microbiota are involved in HCC development [25,26]. *Clostridium* cluster XI produces dichloroacetate, which plays an important role in HCC development via the SASP of hepatic stellate cells (HSCs) [27]. Our study also showed the proportion of fecal *Clostridium* cluster XI was higher in the CDHF + DSS group than in the CDHF group. These results suggest that dietinduced disruption of gut microbiota may promote HCC development.

The liver receives most of its blood supply from the intestine through the portal vein, and is consequently exposed to LPS and pathogen-associated molecular patterns (PAMPs) from the gut. Gäbele E et al. reported that DSS administration enhanced hepatic inflammation and fibrosis in a HF-diet mouse model [28]. Therefore, we added DSS to a CDHF-diet NASH model. Our result showed that DSS administration led to shorter colon length, increased incidence of mucosal changes in the ileum and colon, and aggravated hepatic inflammation and fibrosis relative to the CDHF diet alone. Because we used a CDHF diet, we observed more severe inflammation and fibrosis than in other reported models. In particular, we observed significant elevation of F4/80 in the CDHF + DSS group relative to the CDHF group, indicating that Kupffer cells were more highly activated. It is well known that LPS- and PAMP-activated Kupffer cells release inflammatory mediators, such as tumor necrosis factor (TNF)-α and interleukin (IL)-1β [29–31]. IL-1β from Kupffer cells promotes lipid accumulation and cell death in hepatocytes and fibrogenic responses in HSCs [32]. Our results showed that IL-1β and portal LPS were higher in the CDHF + DSS group than in the CDHF group. Collectively, these findings suggest that elevation of IL-1β and portal LPS induced lipid accumulation and hepatic inflammation and fibrosis in this model. Based on these results, we conclude that induction of intestinal inflammation in NASH may promote hepatic tumorigenesis.

Conflict of interest

The authors report no conflict of interest with regard to this paper.

Acknowledgments

This work was supported in part by a Grant-in-Aid for Scientific Research (26460998) from the Ministry of Education, Culture, Sports, Science and Technology of Japan.

Transparency document

Transparency document related to this article can be found at http://dx.doi.org/10.1016/j.bbrc.2015.12.012.

References

[1] N. Chalasani, Z. Younossi, J.E. Lavine, A.M. Diehl, E.M. Brunt, K. Cusi, M. Charlton, A.J. Sanyal, The diagnosis and management of non-alcoholic fatty liver disease: practice guideline by the American Gastroenterological Association, American Association for the Study of Liver Diseases, and American College of Gastroenterology, Gastroenterology 142 (2012) 1592–1609.
[2] L.A. Adams, J.F. Lymp, J. St Sauver, S.O. Sanderson, K.D. Lindor, A. Feldstein, P. Angulo, The natural history of nonalcoholic fatty liver disease: a population-based cohort study, Gastroenterology 129 (2005) 113–121.
[3] S. Kojima, N. Watanabe, M. Numata, T. Ogawa, S. Matsuzaki, Increase in the prevalence of fatty liver in Japan over the past 12 years: analysis of clinical background, J. Gastroenterol. 38 (2003) 954–961.
[4] C.P. Day, O.F. James, Steatohepatitis: a tale of two ″hits″? Gastroenterology 114 (1998) 842–845.
[5] J.C. Cohen, J.D. Horton, H.H. Hobbs, Human fatty liver disease: old questions and new insights, Science 332 (2011) 1519–1523.
[6] T. Caballero, A. Gila, G. Sanchez-Salgado, P. Munoz de Rueda, J. Leon, S. Delgado, J.A. Munoz, M. Caba-Molina, A. Carazo, A. Ruiz-Extremera, J. Salmeron, Histological and immunohistochemical assessment of liver biopsies in morbidly obese patients, Histol. Histopathol. 27 (2012) 459–466.
[7] F. Caballero, A. Fernandez, A.M. De Lacy, J.C. Fernandez-Checa, J. Caballeria, C. Garcia-Ruiz, Enhanced free cholesterol, SREBP-2 and StAR expression in human NASH, J. Hepatol. 50 (2009) 789–796.
[8] L. Hebbard, J. George, Animal models of nonalcoholic fatty liver disease, Nat. Rev. Gastroenterol. Hepatol. 8 (2011) 35–44.
[9] M.J. Wolf, A. Adili, K. Piotrowitz, Z. Abdullah, Y. Boege, K. Stemmer, M. Ringelhan, N. Simonavicius, M. Egger, D. Wohlleber, A. Lorentzen, C. Einer, S. Schulz, T. Clavel, U. Protzer, C. Thiele, H. Zischka, H. Moch, M. Tschop, A.V. Tumanov, D. Haller, K. Unger, M. Karin, M. Kopf, P. Knolle, A. Weber, M. Heikenwalder, Metabolic activation of intrahepatic CD8+ T cells and NKT cells causes nonalcoholic steatohepatitis and liver cancer via cross-talk with hepatocytes, Cancer Cell 26 (2014) 549–564.
[10] L. Miele, V. Valenza, G. La Torre, M. Montalto, G. Cammarota, R. Ricci, R. Masciana, A. Forgione, M.L. Gabrieli, G. Perotti, F.M. Vecchio, G. Rapaccini, G. Gasbarrini, C.P. Day, A. Grieco, Increased intestinal permeability and tight junction alterations in nonalcoholic fatty liver disease, Hepatology 49 (2009) 1877–1887.
[11] P. Brun, I. Castagliuolo, V. Di Leo, A. Buda, M. Pinzani, G. Palu, D. Martines, Increased intestinal permeability in obese mice: New evidence in the pathogenesis of nonalcoholic steatohepatitis, Am. J. Physiol. Gastrointest. Liver Physiol. 292 (2007) G518–G525.
[12] V. Volynets, M.A. Kuper, S. Strahl, I.B. Maier, A. Spruss, S. Wagnerberger, A. Konigsrainer, S.C. Bischoff, I. Bergheim, Nutrition, intestinal permeability, and blood ethanol levels are altered in patients with nonalcoholic fatty liver disease (NAFLD), Dig. Dis. Sci. 57 (2012) 1932–1941.
[13] K.C. El Kasmi, A.L. Anderson, M.W. Devereaux, S.A. Fillon, J.K. Harris, M.A. Lovell, M.J. Finegold, R.J. Sokol, Toll-like receptor 4-dependent Kupffer cell activation and liver injury in a novel mouse model of parenteral nutrition and intestinal injury, Hepatology 55 (2012) 1518–1528.
[14] D.H. Dapito, A. Mencin, G.Y. Gwak, J.P. Pradere, M.K. Jang, I. Mederacke, J.M. Caviglia, H. Khiabanian, A. Adeyemi, R. Bataller, J.H. Lefkowitch, M. Bower, R. Friedman, R.B. Sartor, R. Rabadan, R.F. Schwabe, Promotion of hepatocellular carcinoma by the intestinal microbiota and TLR4, Cancer Cell 21 (2012) 504–516.
[15] E.J. Park, J.H. Lee, G.Y. Yu, G. He, S.R. Ali, R.G. Holzer, C.H. Osterreicher, H. Takahashi, M. Karin, Dietary and genetic obesity promote liver inflammation and tumorigenesis by enhancing IL-6 and TNF expression, Cell 140 (2010) 197–208.

[16] S. Melgar, A. Karlsson, E. Michaelsson, Acute colitis induced by dextran sulfate sodium progresses to chronicity in C57BL/6 but not in BALB/c mice: Correlation between symptoms and inflammation, Am. J. Physiol. Gastrointest. Liver Physiol. 288 (2005) G1328–G1338.
[17] P.A. Dawson, S. Huxley, B. Gardiner, T. Tran, J.L. McAuley, S. Grimmond, M.A. McGuckin, D. Markovich, Reduced mucin sulfonation and impaired intestinal barrier function in the hyposulfataemic NaS1 null mouse, Gut 58 (2009) 910–919.
[18] K. Nagashima, T. Hisada, M. Sato, J. Mochizuki, Application of new primer-enzyme combinations to terminal restriction fragment length polymorphism profiling of bacterial populations in human feces, Appl. Environ. Microbiol. 69 (2003) 1251–1262.
[19] T. Tanigawa, T. Watanabe, K. Otani, Y. Nadatani, F. Ohkawa, M. Sogawa, H. Yamagami, M. Shiba, K. Watanabe, K. Tominaga, Y. Fujiwara, K. Takeuchi, T. Arakawa, Rebamipide inhibits indomethacin-induced small intestinal injury: possible involvement of intestinal microbiota modulation by upregulation of alpha-defensin 5, Eur. J. Pharmacol. 704 (2013) 64–69.
[20] Y. Nakanishi, K. Murashima, H. Ohara, T. Suzuki, H. Hayashi, M. Sakamoto, T. Fukasawa, H. Kubota, A. Hosono, T. Kono, S. Kaminogawa, Y. Benno, Increase in terminal restriction fragments of *Bacteroidetes*-derived 16S rRNA genes after administration of short-chain fructooligosaccharides, Appl. Environ. Microbiol. 72 (2006) 6271–6276.
[21] C. Bauer, P. Duewell, C. Mayer, H.A. Lehr, K.A. Fitzgerald, M. Dauer, J. Tschopp, S. Endres, E. Latz, M. Schnurr, Colitis induced in mice with dextran sulfate sodium (DSS) is mediated by the NLRP3 inflammasome, Gut 59 (2010) 1192–1199.
[22] S. De Minicis, L. Agostinelli, C. Rychlicki, G.P. Sorice, S. Saccomanno, C. Candelaresi, A. Giaccari, L. Trozzi, I. Pierantonelli, E. Mingarelli, M. Marzioni, G. Muscogiuri, M. Gaggini, A. Benedetti, A. Gastaldelli, M. Guido, G. Svegliati-Baroni, HCC development is associated to peripheral insulin resistance in a mouse model of NASH, PLoS One 9 (2014) e97136.
[23] B. Wang, S.H. Hsu, W. Frankel, K. Ghoshal, S.T. Jacob, Stat3-mediated activation of microRNA-23a suppresses gluconeogenesis in hepatocellular carcinoma by down-regulating glucose-6-phosphatase and peroxisome proliferator-activated receptor gamma, coactivator 1 alpha, Hepatology 56 (2012) 186–197.
[24] V.M. de Lima, C.P. Oliveira, V.A. Alves, M.C. Chammas, E.P. Oliveira, J.T. Stefano, E.S. de Mello, G.G. Cerri, F.J. Carrilho, S.H. Caldwell, A rodent model of NASH with cirrhosis, oval cell proliferation and hepatocellular carcinoma, J. Hepatol. 49 (2008) 1055–1061.
[25] H.L. Zhang, L.X. Yu, W. Yang, L. Tang, Y. Lin, H. Wu, B. Zhai, Y.X. Tan, L. Shan, Q. Liu, H.Y. Chen, R.Y. Dai, B.J. Qiu, Y.Q. He, C. Wang, L.Y. Zheng, Y.Q. Li, F.Q. Wu, Z. Li, H.X. Yan, H.Y. Wang, Profound impact of gut homeostasis on chemically-induced pro-tumorigenic inflammation and hepatocarcinogenesis in rats, J. Hepatol. 57 (2012) 803–812.
[26] J.G. Fox, Y. Feng, E.J. Theve, A.R. Raczynski, J.L. Fiala, A.L. Doernte, M. Williams, J.L. McFaline, J.M. Essigmann, D.B. Schauer, S.R. Tannenbaum, P.C. Dedon, S.A. Weinman, S.M. Lemon, R.C. Fry, A.B. Rogers, Gut microbes define liver cancer risk in mice exposed to chemical and viral transgenic hepatocarcinogens, Gut 59 (2010) 88–97.
[27] S. Yoshimoto, T.M. Loo, K. Atarashi, H. Kanda, S. Sato, S. Oyadomari, Y. Iwakura, K. Oshima, H. Morita, M. Hattori, K. Honda, Y. Ishikawa, E. Hara, N. Ohtani, Obesity-induced gut microbial metabolite promotes liver cancer through senescence secretome, Nature 499 (2013) 97–101.
[28] E. Gabele, K. Dostert, C. Hofmann, R. Wiest, J. Scholmerich, C. Hellerbrand, F. Obermeier, DSS induced colitis increases portal LPS levels and enhances hepatic inflammation and fibrogenesis in experimental NASH, J. Hepatol. 55 (2011) 1391–1399.
[29] M. Darnaud, J. Faivre, N. Moniaux, Targeting gut flora to prevent progression of hepatocellular carcinoma, J. Hepatol. 58 (2013) 385–387.
[30] E. Seki, B. Schnabl, Role of innate immunity and the microbiota in liver fibrosis: Crosstalk between the liver and gut, J. Physiol. 590 (2012) 447–458.
[31] T. Luedde, R.F. Schwabe, NF-kappaB in the liver–linking injury, fibrosis and hepatocellular carcinoma, Nat. Rev. Gastroenterol. Hepatol. 8 (2011) 108–118.
[32] K. Miura, Y. Kodama, S. Inokuchi, B. Schnabl, T. Aoyama, H. Ohnishi, J.M. Olefsky, D.A. Brenner, E. Seki, Toll-like receptor 9 promotes steatohepatitis by induction of interleukin-1beta in mice, Gastroenterology 139 (2010) 323–334 e327.